PCCP

Accepted Manuscript

ROYAL SOCIETY OF CHEMISTRY

www.rsc.org/pccp

Spectroscopic and Photophysical Study of the Demetallation of a Zinc Porphyrin and the Aggregation of its Free Base in a Tetraalkylphosphonium Ionic Liquid

Neeraj K. Giri, Abhinandan Banerjee, Robert W. J. Scott, Matthew F. Paige,* and Ronald P. Steer*

Department of Chemistry

University of Saskatchewan

Saskatoon, Saskatchewan,

Canada S7N 5C9

* to whom correspondence should be addressed

email: ron.steer@usask.ca

matthew.paige@usask.ca

Keywords: metalloporphyrin demetallation, ionic liquids, free base porphyrin, porphyrin J aggregates, thermal equilibrium, photophysics

Abstract:

Dissolving zinc tetraphenylporphyrin in the tetraalkylphosphonium chloride ionic liquid P4448Cl results in progressive demetallation of the solute and quantitative production of the free base porphyrin. Aggregation of the free base occurs in which the monomer and J aggregates are in fully reversible thermal equilibrium in the ionic liquid. The thermodynamic, kinetic and spectroscopic behaviour of this system is described based on absorption, emission and excited state lifetime measurements. Both the thermodynamics of the ground state aggregation and the kinetics of the excited state relaxation processes are unusual due to the particular role played by the ionic liquid solvent.

Introduction:

Room temperature ionic liquids (ILs) are attractive alternatives to common molecular organic solvents for a multitude of reasons that have been thoroughly discussed in recent reviews.[1-6] The profusion of new ILs having a wide variety of tailorable properties has resulted in a progression of these materials from academic curiosities with specialized electrochemical applications to viable media for use in numerous industrial processes. Determining and correlating the behaviour of families of solutes in ILs has therefore now become a vast arena for research.

Of particular interest in the development of low-cost, efficient organic photovoltaic cells (OPVs) is the fact that IL solvents not only have immeasurably low volatilities at room temperature, but also exhibit exceedingly small oxygen solubilities, large ionic mobilities and can exhibit a wide four to six volt electrochemical window.[1,3,6] Because they mimic photosynthesis, porphyrins and their metallated derivatives are prominent among the materials chosen for use as primary photon absorbers in OPVs; their behaviour in ILs[7-11] that could be used as electrolytes in these cells is therefore of considerable interest. The relevant properties of a common model metalloporphyrin, zinc tetraphenylporphyrin (ZnTPP), in an imidazolium IL have been established.[12] In this case, the metalloporphyrin exhibited an unusually small molar absorptivity in the IL, but otherwise was stable and exhibited photophysical properties in accord with correlations based on molecular solvents. Phosphonium-based ILs, however, have not been examined as potential media in OPVs despite the facts that: (i) they are

relatively easy to purify (and have impurities that do not fluoresce significantly in the visible region of the spectrum); (ii) they exist in the liquid phase at temperatures significantly lower than room temperature, and (iii) they exhibit good solubility for a wide range of both ionic and non-ionic solutes, including porphyrins.[13-15]

Porphyrins aggregate in many media. Two types of highly-ordered aggregates in fluid solvents and polymer hosts are well-known; (i) H-aggregates in which the porphyrin macrocycles π-stack in a perpendicular face-to-face array, and (ii) J-aggregates in which the monomers exhibit a "slipped-deck-of-cards" geometry leading to a side-by-side arrangement in the slippage limit.[16-18] The two distributions can be easily distinguished spectroscopically, with H-aggregates exhibiting a hypsochromic shift and J-aggregates a bathochromic shift in their UV-visible absorptions relative to their constituent monomers. In aqueous fluid media containing surfactants, a variety of equilibria among dianionic porphyrin monomers in bulk solution, monomers in micelles and H- and J-aggregates in micelles have been characterized.[19] In some ILs, a number of stacked aggregates in which the solvent aromatic cation participates in the aggregated structure have been identified computationally.[20]

The state and degree of aggregation of porphyrins in ILs are of considerable interest in OPVs based on these systems because these are important factors that determine their overall energy conversion efficiency.[7,11,21] Aggregation is also of particular importance in developing improved OPV efficiencies via non-coherent

photon upconversion (NCPU). The most promising of the NCPU processes involves electronic energy pooling by triplet-triplet annihilation (TTA) where, in the system we are investigating, the porphyrin plays the dual role of absorber and photon upconverter.[12,22,23] Inefficiencies in such systems are introduced by the requirement that two upconverter triplet excitons interact at van der Waals distances.[24] If, due to intermolecular exciton diffusion, times between absorption and TTA are long compared with triplet exciton lifetimes, a significant fraction of the absorbed solar energy will be lost as heat. On the other hand, if fast intramolecular energy transfer from antennae to an upconverting aggregate can be constructed, diffusional losses should be minimized.

In order to provide guidance for the possible use of porphyrins and ILs in OPVs, we report here a study of the spectroscopic and photophysical behaviour of zinc tetraphenylporphyrin (ZnTPP) and its free base (H_2TPP) in the P4448Cl tetraalkylphosphonium chloride IL, which is typical of the phosphonium IL series. Demetallation of the metalloporphyrin and aggregation of the resulting free base are described and the implications for OPVs are discussed.

Experimental Section:

Materials: Purification of the IL

Tributyl(octyl)phosphonium chloride (CYPHOS® 253) was purchased from Cytec Ltd. and subjected to a purification regimen similar to that used by Earle, *et*

al.[25] for imidazolium ionic liquids, as described in detail in the Supporting Information. ^{1}H NMR spectroscopy of the purified IL in $CDCl_3$ failed to reveal impurities (Fig. S1), but trace water would not have been observed. Nevertheless, the purified IL exhibited weak absorbance due to trace impurities throughout the visible region, rising gradually to an absorbance of greater than 0.01 in a 1 cm cell at $\lambda < 410$ nm (Fig. S6). This background was subtracted from all absorption spectra but the luminescence produced as a result of the rising absorbance prevented clean emission spectra and emission lifetimes to be determined at excitation wavelengths further into the violet and ultraviolet range.

Preparation of solutions

meso-Tetraphenylporphine zinc (ZnTPP, Alfa Aesar) and free base tetraphenylporphine (H_2TPP, Avocado) were used as received. Solutions of the porphyrins in P4448Cl were prepared by a method similar to that employed by Murakami[26,27] in which the rate of dissolution of the solute in the IL is increased by first dissolving the solid in a small amount of a volatile solvent. Stock solutions of the porphyrins in dichloromethane (DCM, EM Science) were prepared and the required amounts injected into the IL and stirred. Continuous pumping while stirring at 60°C under vacuum for several hours removed the majority of the DCM and other volatile impurities. The last traces of volatile materials were removed by repeatedly cycling the solutions between room temperature and 100°C until the spectra exhibited no further change at a given temperature (*vide infra*).

Instrumentation

Absorption spectra at temperatures between 0°C and 100°C were taken with a Varian Cary 6000i UV-Vis spectrophotometer equipped with a variable temperature sample holder. Steady state emission spectra were measured with a PTI QuantaMaster spectrofluorometer. Fluorescence lifetimes were measured by time-correlated single-photon counting (TCSPC) as described in detail previously.[28] Decay parameters were obtained by using a non-linear least squares iterative convolution process based on the Marquardt algorithm, with the reduced χ^2 value and the distribution of the weighted residuals as goodness-of-fit measures.

Results and Discussion:

Initial experiments employed ZnTPP, as the intent was to determine the suitability of the tetraalkylphosphonium chloride IL as a solvent in model upconversion experiments for solar photovoltaic cells.[7,12] Addition of a small amount of a dilute solution of ZnTPP in dichloromethane to the P4448Cl IL resulted in an immediate colour change from purple to green in the two-phase mixture. Removal of the DCM solvent under vacuum resulted in a further colour change. Continuous evacuation at 60°C until no further solvent removal was evident resulted in the UV-visible absorption spectra shown in Figure 1 as a function of temperature. In this example, the resulting solution is dilute, 2.5 μM porphyrin in the IL. The Soret region of the spectrum is particularly revealing, where three strong bands with maxima near 419 nm, 436 nm and 452 nm are observed. The intensity

variations with temperature of these bands are reversible and a thermal isosbestic point is observed at 430 nm.

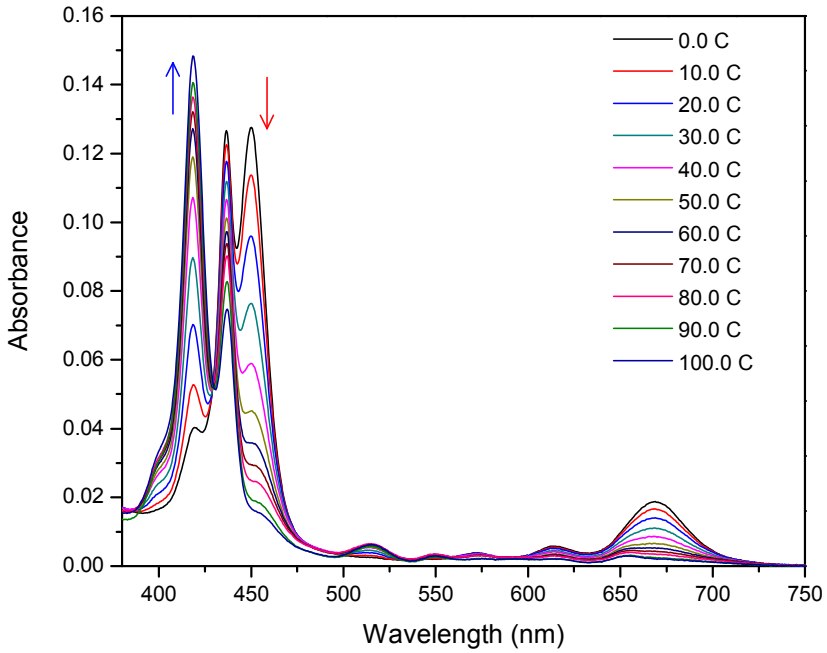

Figure 1: Absorption spectra of 2.5 μM porphyrin in P4448Cl. These spectra were taken in a sealed cuvette after initial removal of dichloromethane under vacuum. Arrows show the trends as the temperature increases.

On the basis of previous spectroscopic evidence,[29] it would be tempting to assign these three features to H aggregates, monomer, and J aggregates of ZnTPP respectively in the IL. However, opening the cuvettes and cycling the IL solutions repeatedly between 0°C and 100°C resulted in irreversible changes in the spectra. After 10 such cycles, the central band in the Soret region at 436 nm disappeared and the spectra then remained entirely fully reversible with changing temperature, with the isosbestic point remaining at 430 nm, as shown in Figure 2A.

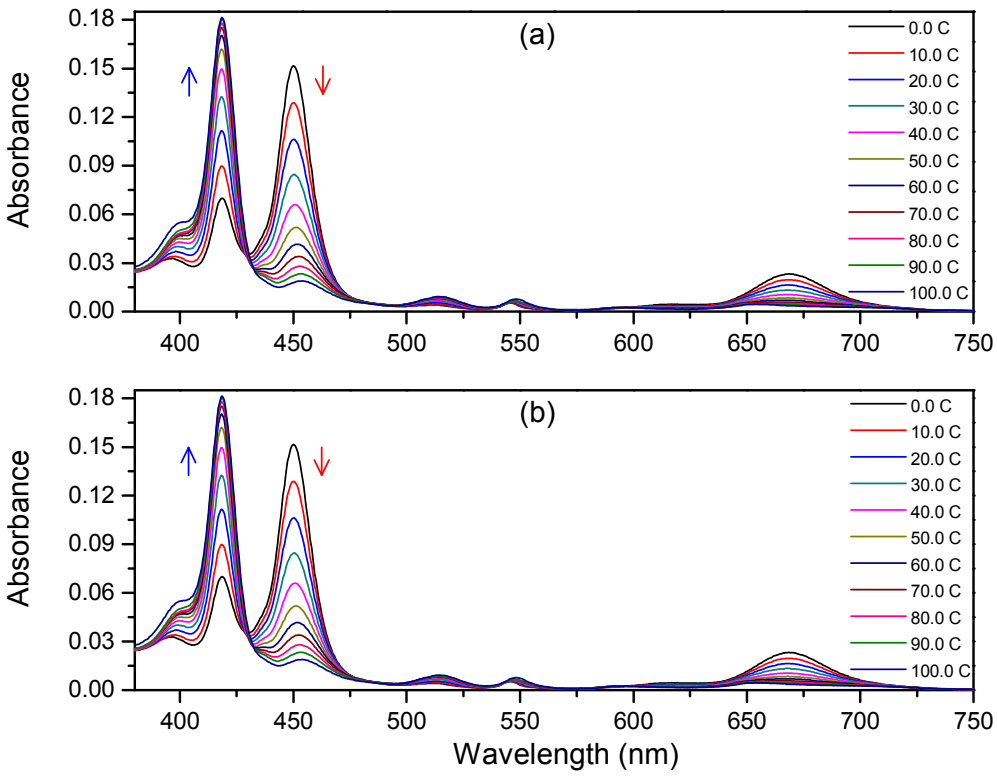

Figure 2: (A) Absorption spectra of 2.5 μM ZnTPP in P4448Cl. The sample in the IL was subjected to prolonged pumping under vacuum at 60 °C and ten temperature cycles from 0°C to 100°C prior to taking these spectra. (B) Absorption spectra of 2.5 μM H_2TPP in P4448Cl, prepared in the same way as for (A). The observed changes are fully reversible. The background due to the IL has not been subtracted in these spectra.

We attribute these observations to the progressive demetallation[30,31] of the ZnTPP solute in the IL and the quantitative production of its free base, H_2TPP, as the last traces of the dichloromethane solvent are driven off during temperature cycling. Such a process would require the presence of a proton donor, most likely water or residual acid from the IL preparation, at a concentration in substantial excess of the porphyrin. Water is a common impurity that is difficult to remove completely in ILs, so the quantitative production of the free base porphyrin in this system, where the solute is present in only ppm quantities, is entirely feasible. Further deliberate

addition of water to the system produced no significant change. Protonation of the free base does not occur, however, because the Q band spectra exhibit features characteristic of the D_{2h} H_2TPP species,[31] not the D_{4h} macrocycle of H_4TPP^{2+}, at all concentrations of the porphyrin in the IL (*vide infra*). The net reaction is therefore most likely $ZnTPP + 2\ H_2O \rightarrow H_2TPP + Zn(OH)_2$ with the possible formation of a number of additional species, $Zn(OH)_xCl_y$ in this IL.

After the demetallation process is complete, the IL solution exhibits spectra characteristic of the free base monomer at high temperatures and primarily its J aggregates at low temperatures within the 0°C to 100°C range explored. The changes with varying temperature are fully reversible. Behaviour identical to that of Figure 2A was observed by dissolving the free base porphyrin, H_2TPP, directly in the IL, as demonstrated in Figure 2B.

To interpret quantitatively the behaviour of the porphyrin in the IL, the spectra of the dilute solutions of both ZnTPP and H_2TPP were modeled on a wavenumber scale as a sum of Gaussian bands. However, for the sake of consistency only the data from experiments in which H_2TPP was dissolved directly in the IL were employed in further analysis of the solute's photophysical properties. Representative fits for the H_2TPP in P4448Cl are shown in Figure 3 for the Soret region and the complete sets of data are provided in the Supporting Information (Figures S2, S3 and Tables S1, S2). The strong, narrower band near 23890 cm^{-1} (418.6 nm) is assigned as the Soret band of monomeric H_2TPP based on previous

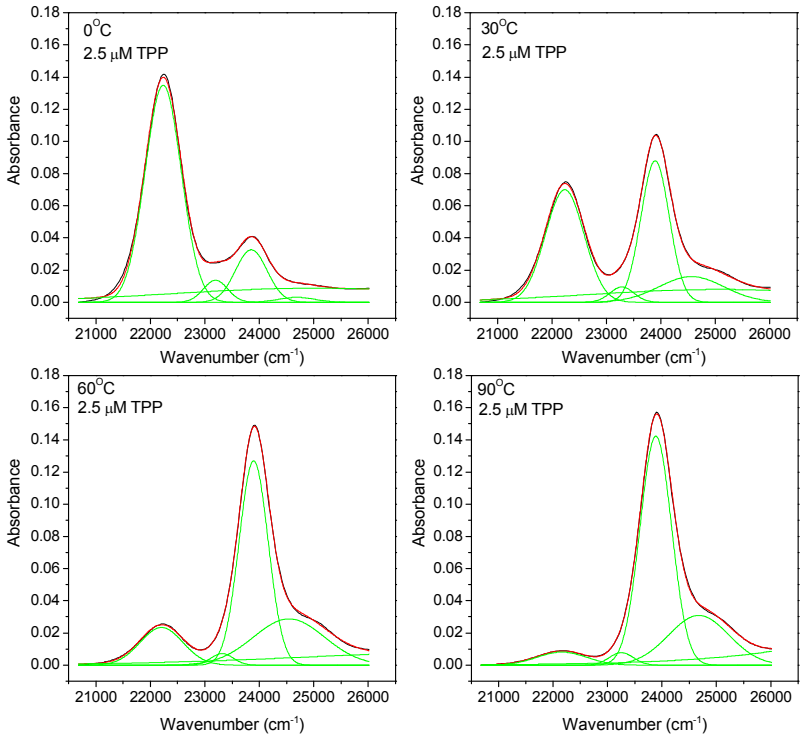

Figure 3: Gaussian band shape fits to the spectra of Figure 2B in the Soret region as a function of temperature. Weak background absorbance due to the IL alone has been subtracted in all cases.

studies of the free base porphyrin in a variety of media.[32,33] This assignment is supported by measurements of fluorescence lifetimes (*vide infra*). The feature to the red near 22220 cm^{-1} (450.0 nm) increases in intensity at lower temperatures at the expense of the band at 23890 cm^{-1} and is assigned to the J aggregate of the H_2TPP. The latter assignment is consistent with previous observations of the aggregation behaviour of porphyrins in both molecular solvents and other ILs, although the bathochromic shift is rather smaller than in other media.[16-19] The reversible interconversion of these two features as a function of changing temperature and the presence of a single isosbestic point at 430 nm in this spectral region suggest that

the monomer and aggregate are in thermal equilibrium under these conditions in the IL.

The fit of multiple Gaussian features to the spectra in the Soret region reveals an additional weak band to the blue of the prominent free base monomer band at 23890 cm^{-1}. Forcing a single Gaussian to model this feature and deconvoluting it from the measured spectra is subject to greater error than other bands not only because it is weak, but because the IL background is substantially greater in this region (*cf*. Supporting Information). Nevertheless, one can identify several qualitative properties of this feature: (i) it is considerably weaker than the main Soret band, (ii) it is significantly broader (by about a factor of two) than the main Soret band, (iii) its apparent separation from the main Soret band decreases with increasing temperature, and (iv) its relative intensity increases with increasing temperature. (Refer to the Supporting Information (Fig. S2, Table S1) for details.) In molecular solvents at room temperature, a similar feature has been assigned[32,33] to a vibronic band, B(1,0), spaced some 1250 cm^{-1} from the origin, B(0,0), with the greatest Franck-Condon activity assigned to totally symmetric ring stretching modes,[34] consistent with the fully-allowed nature of the Soret transition. The behaviour of this feature as a function of temperature in the IL suggests that additional hot band transitions, B(1,1), may contribute to the absorbance in this region, thereby increasing the relative intensity of the feature(s) to the blue of B(0,0) with increasing temperature and decreasing its apparent spacing from B(0,0) in the forced Gaussian fit. Placing an additional Gaussian, labelled B(1,1), with

temperature sensitive amplitude between fixed Gaussians at B(0,0) and B(1,0) quantitatively reproduces the observed trends.

If we assume, on the basis of the above analysis, that the H_2TPP monomer is in thermal equilibrium with its J aggregate(s), a van't Hoff plot should yield a quantitative measure of the enthalpy difference between the solvated aggregate (J) and its solvated monomer (M) constituents. Thus, the equilibrium is nM ⇆ J with temperature-dependent equilibrium constant $K_{eq} = [J]/[M]^n$. The magnitude of the spectral shift of the Soret absorption band from monomer to aggregate suggests that n = 2, based on previous calculations and observations in molecular solvents.[35,36] This assumption is consistent with the observed mass balance demanded by a dimerization equilibrium, as shown in the Supporting Information for the dilute solution. Based on this assumption, and using the areas under the Gaussian fits for the Soret bands of the monomer (total of B(0,0), B(1,0) and B,(1,1)) and the J aggregate as measures of their relative concentrations, the data of Figure 3 then produce the van't Hoff plot shown in Figure 4. The slope provides ΔH = –71.4 ± 0.9 kJ mol^{-1} for the stabilization of the dimeric solvated J aggregate of H_2TPP in the P4448Cl IL. The unusually large magnitude of this enthalpy change[37] suggests that the solvation energy in the IL is greater than that expected in most non-hydrogen bonding molecular solvents and is discussed later.

We note that the least accurate K_{eq} data occur at the extremes of the 0 to 100 ˚C temperature range employed in this experiment. Nevertheless, although a linear

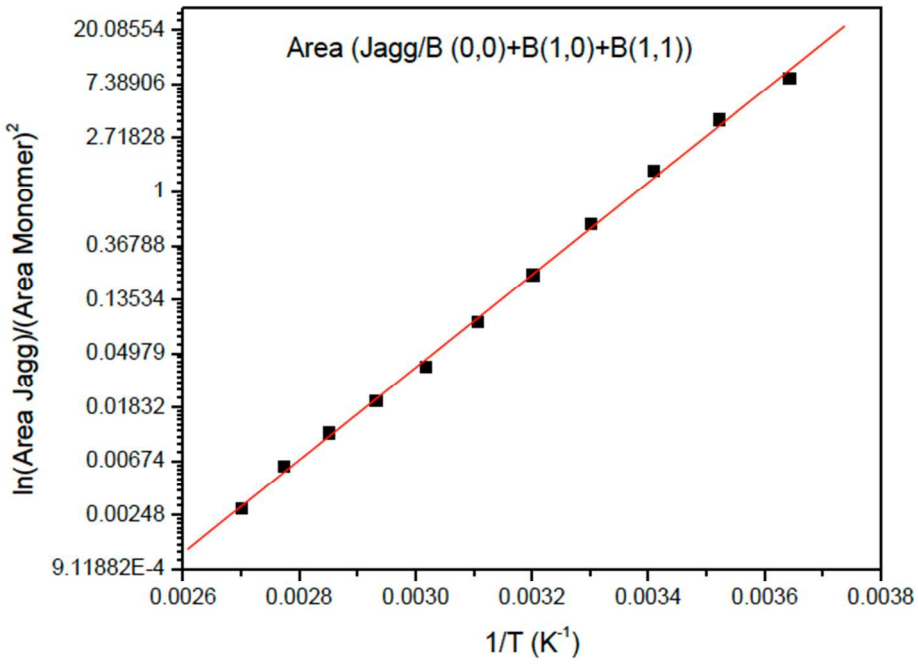

Figure 4: Van't Hoff plot for the 2 M ⇆ J equilibrium of 2.5 μM H_2TPP in the P4448Cl ionic liquid, assuming n = 2. The area of the Soret band is taken as the sum of the areas of three peaks B(0,0), B(1,0) and B(1,1). The slope of the line gives the value $\Delta H = -71.4 \pm 0.9$ kJ mol^{-1}.

correlation is forced in Figure 4, slight curvatures in this van't Hoff plot at the extrema are possible within the measured error limits. At larger starting concentrations of porphyrin in the IL, these absorption spectra and their variations with changing temperature remain similar to those shown above for the 2.5 μM porphyrin concentration, and the modeled areas under each band scale linearly with increasing concentration at each temperature. However, every Gaussian band broadens with increasing solute concentration, the maxima shift slightly and van't Hoff plots similar to Figure 4 become clearly non-linear at the highest porphyrin concentrations employed (25 μM, *cf.* Supporting Information (Fig. S4)), all of which

suggest that higher aggregates may be forming and becoming more prevalent at higher porphyrin concentrations in the IL.

Further thermodynamic data regarding the aggregation process can be obtained if a reliable value of the dimerization equilibrium constant, K_{eq}, can be obtained. Using the requirements of the mass balance and the resulting conclusion that the J aggregates have an oscillator strength that is approximately a factor of 2 larger than that of the monomer (Supporting Information) leads to the conclusion that value of K_{eq} at 298 K is close to 4 x 10^5 when the dilute solution of H_2TPP (2.5 μM) in the IL is employed. Thus $\Delta G° = - RT\ell n(K_{eq}) = -$ 32 kJ mol^{-1} and $\Delta S° = -130$ J K^{-1} mol^{-1} at 298 K. This value of $\Delta G°$ is similar to those obtained for the dimerization of other porphyrins in aqueous media.[37] The sign of $\Delta S°$ is consistent with the nature of the aggregation process but its magnitude is unusually large,[37] likely indicating that dimerization in the IL involves considerable solvent ordering.

The absorption spectra of this system in the Q band region (Figures 2 and 5) are more complex. Three well-resolved bands at 515, 549 and 668 nm and a number of other weaker features are observed. Those at 515 and 549 nm increase in intensity with increasing temperature whereas that at 668 nm and its shoulder at 617 nm decrease. At the highest temperatures the latter features are sufficiently attenuated to reveal two weaker underlying bands at *ca.* 652 and 595 nm, which increase in relative intensity with increasing temperature. Two clear thermal isosbestic points appear at 562 and 597 nm. These Q band features also exhibit completely reversible changes as a function of temperature when the spectra are

measured in a closed cuvette. Different starting porphyrin concentrations result in similar spectra throughout the UV-visible region, but with slightly shifted band maxima and substantially shifted relative intensities.

Modeling the dilute solution spectra in this region by a sum of Gaussians results in the data plotted in Figure 5. An additional very weak feature on the red side of the strong 668 nm band appears in the model. This band increases with

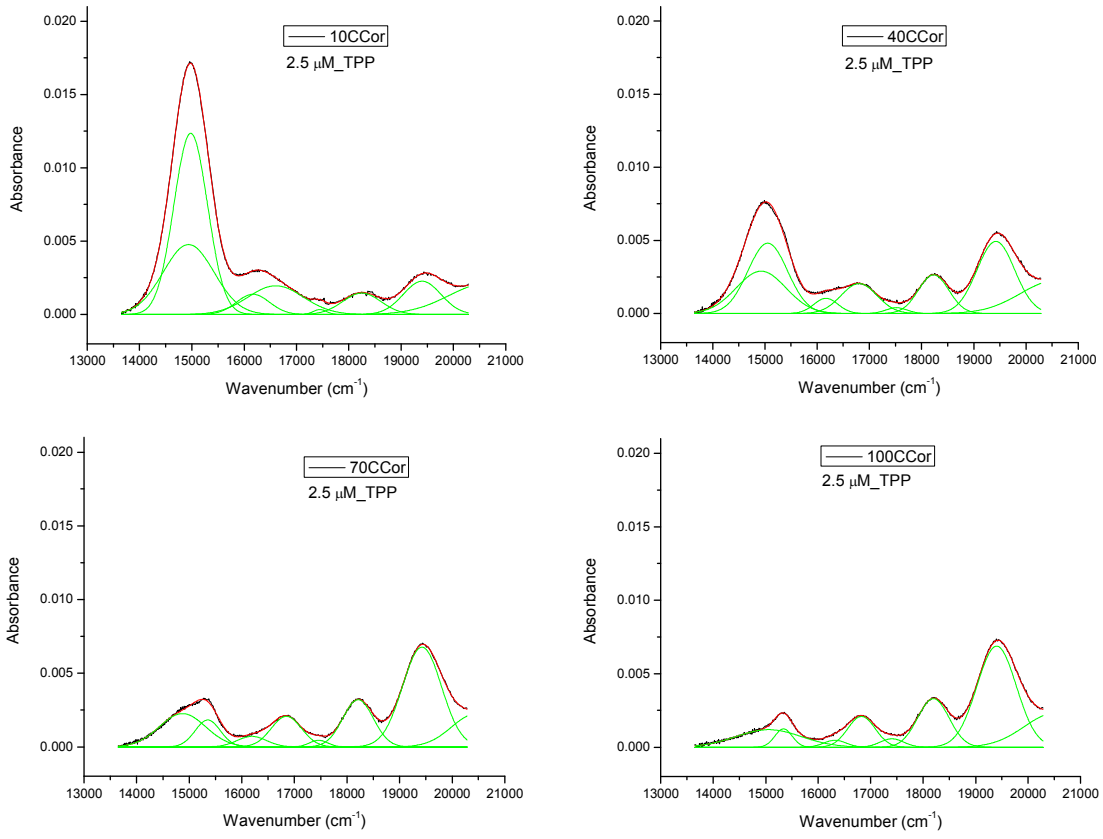

Figure 5: Gaussian band shape fits to the absorption spectra of H_2TPP in the Q band region as a function of temperature (10, 40, 70 and 100 °C). Weak background absorbance due to the IL alone has been subtracted.

increasing temperature, but at a rate that is quantitatively different from all of the others. It is therefore assigned as a hot vibronic band and is not included in further analysis. The full set of data is provided in the Supporting Information (Figure S5 and Table S3).

Distinctly different fluorescence spectra, Figure 6, were observed when exciting in the strong Soret band features due to the J aggregates (λ_{ex} = 458 nm, on the red side of the maximum to minimize overlap) compared to those of the monomer (λ_{ex} = 414 nm, on the blue side of the maximum). Completely clean excitation of the monomer and its aggregates was not possible due to overlap of their Soret bands. Nevertheless, the features due to each species are clearly distinguishable. Excitation of the J aggregates at 458 nm produces only one broad,

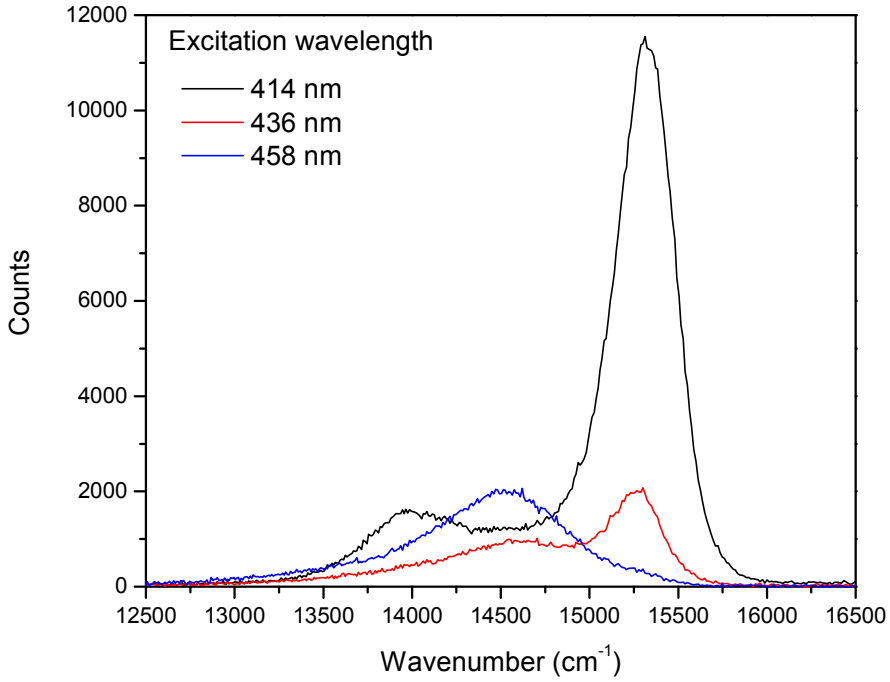

Figure 6: Fluorescence spectra in the Q band region resulting from excitation at 414 nm, 436 nm and 458 nm.

relatively weak emission band with a maximum near 690 nm (14500 cm^{-1}) whereas excitation of the H_2TPP monomer at 414 nm produces two bands, a strong feature at 654 nm (15300 cm^{-1}) and a weaker band some 1450 cm^{-1} further to the red at *ca.* 720 nm. Excitation at a wavelength of 436 nm between the two strong Soret bands produces an emission spectrum that is a composite of the other two.

Previous reports concerning the absorption spectra of free base tetraphenyl-porphyrin in both molecular solvents[32,33] and ILs[38] leads one to expect that the absorption spectrum in the Q band region will consist of four well-defined bands ($Q_x(0,0)$, $Q_x(1,0)$, $Q_y(0,0)$, $Q_y(1,0)$ the last of these with one weak shoulder to the blue) whereas the emission spectrum will exhibit two bands ($Q_x(0,0)$, $Q_x(0,1)$ plus a weak hot band, $Q_x(1,0)$). The fluorescence intensity of a J aggregate is expected to be weaker than that of its constituent monomers due to enhanced radiationless decay in the excited aggregate, and the spectrum sometimes is not observed at all. Nevertheless fluorescence emission previously attributed to J aggregated porphyrins has been reported to consist of one broad feature.[36,38,39] Using these previous reports as a guide, and employing the observed temperature sensitivities of each modeled absorption feature, the Q band absorption and emission spectra are assigned as follows. First, the $S_1 - S_0$ origin of the free base monomer can be unequivocally located from the $Q_x(0,0)$ emission band at 654 nm obtained by exciting in the H_2TPP monomer Soret band at 414 nm. This, together with its companion weaker $Q_x(0,1)$ fluorescence band at 720 nm, some 1450 cm^{-1} to the red of the origin, agrees completely with the locations, relative intensities and spacing of these two bands of H_2TPP in a variety of media.[32-34] Excitation in the broad feature

in the Soret region assigned to J aggregates of H_2TPP produces a single broad band in the Q band emission spectrum, with a maximum near 690 nm. The $S_1 - S_0$ origin of the J aggregate's emission spectrum must lie on the blue edge of this broad feature, placing it near the maximum of the $Q_x(0,0)$ emission band of the monomer at 654 nm.

The four strongest features in the Q absorption region of the D_{2h} monomer are expected to diminish in intensity in the order $Q_y(1,0) > Q_y(0,0) > Q_x(1,0) > Q_x(0,0)$.[32,33] The two strong bands at 515 nm and 549 nm, which increase in relative intensity with increasing temperature, are thus assigned as $Q_y(1,0)$ and $Q_y(0,0)$. Known spacings between the Q_y and Q_x bands in a variety of media therefore should place the $Q_x(1,0)$ and $Q_x(0,0)$ bands in the absorption spectra near 590 nm and 645 nm respectively. Thus the weak underlying feature at 595 nm, which increases in relative intensity at the higher temperatures, is assigned to $Q_x(1,0)$. This would then place the weakest $Q_x(0,0)$ absorption band near 650 nm, in agreement with the known location of the $Q_x(0,0)$ band at 654 nm in the fluorescence spectrum and the location of the weak feature in the absorption spectrum at 652 nm uncovered at high temperatures.

The Soret and Q band data thus provide interesting information concerning the excitonic coupling energies in the J aggregate. Using absorption maxima to locate excited state energies, the Soret monomer-to-J aggregate spacing is approximately 1670 cm^{-1} whereas the same spacing in the Q band region is *ca*. 370 cm^{-1} (although the latter number is subject to significantly larger error due to the overlap of

spectral features in this region). The excitonic splitting exhibited in the Q bands is thus a factor of 4 to 5 times smaller than that in the Soret bands, qualitatively consistent with the relative magnitudes of the oscillator strengths of these transitions and the requirements of excitonic coupling theory.[39,40]

In principle it should be possible to provide further confirmation of these assignments by measuring the lifetimes of the fluorescence excited in the various Soret bands and observed at the Q band emission maxima. Fortunately, excitation in the violet where the H_2TPP monomer absorbs and the IL begins to absorb more strongly (Figure S6) produces background fluorescence of the IL itself that is orders of magnitude smaller than that of the porphyrin; excitation at 414, 436 nm and 458 nm produced useful data. The temporal decay curves are provided in the Supporting Information (Fig. S7) and the data extracted from them using bi- and tri-exponential fits are reported in Table 1. In all cases, excitation at room temperature in the Soret

Table 1: Lifetimes of the S_1 state of 2.5 μM H_2TPP aggregated in P4448Cl at room temperature, measured at different excitation (458, 436 and 414 nm) and emission wavelengths (652, 693 and 716 nm). Numbers in parentheses show the fraction of each species decaying with a particular time constant obtained from the expression $F_x = a_x\tau_x/\Sigma a_i\tau_i$.

Emission Wavelength	**Excitation Wavelength**								
	458 nm			**436 nm**			**414 nm**		
	τ_1 (ns) (F_1)	τ_2 (ns) (F_2)	τ_3 (ns) (F_3)	τ_1 (ns) (F_1)	τ_2 (ns) (F_2)	τ_3 (ns) (F_3)	τ_1 (ns) (F_1)	τ_2 (ns) (F_2)	τ_3 (ns) (F_3)
652 nm				0.60 (0.01)	3.08 (0.06)	9.16 (0.93)	9.27 (0.92)	2.92 (0.08)	
693 nm	0.60 (0.09)	1.87 (0.71)	5.34 (0.20)	1.98 (0.34)	0.37 (0.03)	8.90 (0.64)			
716 nm							9.76 (0.88)	1.85 (0.12)	

region and observation at the maxima of the strong bands in the Q band emission spectra produced multi-exponential fluorescence decay. However, excitation of the monomer at 414 nm and observation of its fluorescence at 652 nm and 716 nm where overlaps with the absorption and emission of the J aggregate at room temperature are minimized leads to a near mono-exponential decay with an average lifetime of 9.4 ns. This value is only slightly smaller than the average value of the fluorescence lifetime of the $S_1(Q_x)$ state obtained for H_2TPP in undegassed molecular solvents at room temperature.[41,42]

Excitation of the J aggregate on the red side of its Soret absorption at 458 nm and observation of its Q band emission at 693 nm yields a triple exponential decay with lifetimes, τ, and fractional fluorescence yields, (F), of 0.6 ns (0.09), 1.9 ns (0.71) and 5.3 ns (0.20). The major component should be assigned to the dimer aggregate, but its lifetime is a factor of about six longer than those of J aggregates in other media, particularly aqueous solutions of high ionic strength where the J aggregate has a lifetime of *ca.* 0.3 ns.[43] Nevertheless, the intensity of the J aggregate emission band relative to that of the monomer (*ca*. 1:6, Fig. 6) is consistent with a fluorescing S_1 excitonic state that has a measured lifetime of 1 to 2 ns, as observed. This species also has a lifetime that is very similar to those of covalently tethered but weakly interacting free-base porphyrin dimers.[44] The major 1.9 ns component in the three-component decay is thus assigned to the J-aggregated dimer.

The fact that the J aggregate's S_1 fluorescence intensity and lifetime are significantly larger than those found in polar molecular solvents is consistent with a

slower rate of radiationless decay of the aggregate's exciton in the IL, and thus suggests that the strength of the interaction between the porphyrins is diminished in the aggregate by strong solvation effects. This interpretation is also consistent with the observed magnitude of the Soret band excitonic splitting (1670 cm^{-1} if solvation energy differences between ground and excited states are ignored), which is significantly smaller than observed in molecular solvents.[38-41]

The minor sub-nanosecond component in the three-component fit is perhaps suggestive of absorption and emission by a small fraction of larger aggregates whereas the 5.3 ns component suggests that dissociation of the initially excited dimer aggregate takes place on a time scale that is similar to its ns lifetime, much like exciplexes.[45] The latter suggestion is consistent with the distance a porphyrin molecule would diffuse in a few ns to remove it from effective interaction with its dimeric partner. Excitation of the room temperature solution at 436 nm where both monomer and J aggregate absorb significantly results in multi-exponential decay, favouring the 9.4 ns component of the monomer when observing at 652 nm and producing a much larger 1.9 ns contribution when observing at 693 nm. All of these observations are consistent with the previous spectroscopic assignments of the Soret band absorptions and the Q band emissions.

The exceptionally large magnitude of $\Delta H = -71.4 \pm 0.9$ kJ mol^{-1} obtained from the van't Hoff plots begs further discussion. Such a value of ΔH is too large to be associated solely with the non-covalent interaction between two uncharged, non-polar H_2TPP molecules. For example, the dimerization of deuteroporphyrin in

aqueous neutral buffered saline solution yields a value of $\Delta H = -46.0$ kJ mol^{-1}.[37] Thus the exceptionally large enthalpy change observed in the IL must reflect a difference in total solute plus solvent interaction energy for the aggregated dimer relative to its constituent monomers. Indeed, the fact that ZnTPP is known to be perfectly stable in imidazolium ILs[12] but is demetallated in P4448Cl at room temperature indicates that solute-solvent interaction is significantly stronger in the present system.

If the value of $\Delta H = -71.4 \pm 0.9$ kJ mol^{-1} (stabilization of 5970 cm^{-1} per dimer molecule) is applied only to the ground state of the aggregating system, then the observed red-shifts in the Soret and Q band spectra associated with aggregation (1670 cm^{-1} and 370 cm^{-1} respectively, in a ratio of the correct order of magnitude) would make no sense. Rather, we will assume that a similar solvation effect is also applicable to the observed excited states so that the excitonic stabilzation energies obtained from the red-shifts of the Soret and Q bands remain qualitatively reasonable. We then ask if there is a plausible explanation for such a large solvation effect.

Calculations that place cations from the IL within van der Waals distances of the free base porphyrin moiety indicate that unusually large solvation energies are possible. For example, using a polarizable force field method Cao *et al*.[18] demonstrate that π-stacking of imidazolium cations on either side of a single free base porphyrin yields an unusually stable slipped-deck-of-cards structure with a solute-solvent binding energy of the order of 100 kJ mol^{-1}. Moreover, the binding energy thus calculated is greater than the binding energy between the cation and

anion of the IL alone (in that case $BMIM^+$ and PF_6^-). Although the π-π component of the cation-porphyrin interaction will not be present in the tetraalkyphosphonium IL used here, the magnitude of the stabilization calculated per mole of free base porphyrin is nevertheless in keeping with the measured magnitude of ΔH from the van't Hoff plots. Chloride anion stabilization of the aggregate cannot be ruled out altogether, but seems less likely given that anion effects are most prominent in cationic porphyrin aggregation.[46]

Conclusions:

Demetallation of ZnTPP occurs when it is dissolved in a P4448Cl IL and cycled under vacuum between 0 °C and 100 °C. A quantitative yield of the free base porphyrin is produced, most likely by reaction with trace impurity water. The free base participates in an unusual, fully reversible equilibrium in which the monomer dominates at high temperature and a dimeric J aggregate at low temperature. The thermodynamic functions characterizing the ground state equilibrium reveal an unusually large enthalpy change for the dimerization in the IL, consistent with a strong solute-solvent interaction.

The absorption and fluorescence emission spectra of both the monomer and the J aggregate have been analyzed and their excited state kinetics determined via time-dependent fluorescence measurements. Both the spectroscopic and kinetic measurements reveal unusual solvation effects attributable to this particular ionic liquid and not found in those of the imidazolium series. In particular the strong solvation effects reduce the excitonic interaction energy in the J aggregate resulting

in a red-shift of the Soret absorption band that is unusually small and a radiationless decay rate of the singlet exciton that is unusually slow. The unusual solvation effects of this IL are thus reflected consistently in both the ground state thermodynamics and the excited state kinetics of this system.

Despite many favourable properties, tetraalkylphosphonium ionic liquids appear not to be suitable for OPVs in which metalloporphyrins are the primary solar energy absorbers.

Acknowledgements:

The authors are pleased to acknowledge the continuing support of this research by the Natural Sciences and Engineering Research Council of Canada.

References:

1. A. E. Visser, N. J. Bridges and R. D. Rogers, (Eds.), Ionic liquids: science and applications, *ACS Symp. Ser.* 2012, **1117**, and articles therein.

2. M. Smiglak, J. M. Pringle, X. Lu, L. Han, S. Zhang, H. Gao, D. R. MacFarlane and R. D. Rogers, Ionic liquids for energy, materials and medicine, *Chem. Comm.*, 2014, **50**, 9228-9250.

3. J. Le Beau, L. Viau and A. Vioux, Ionogels: ionic liquid based hybrid materials, *Chem. Soc. Rev.*, 2011, **40**, 907-925.

4. H. Passos, M. G. Freire and J. A. P. Coutinho, Ionic liquid solutions as extractive solvents for value-added compounds from biomass, *Green Chem.*, 2014, DOI: 10.1039/c4gc00236a.

5. S. Zhang, J. Sun, X. Zhang, J. Xin, Q. Miao and J. Wang, Ionic liquid-based green processes for energy production, *Chem. Soc. Rev.* 2014, DOI: 10.1039/c3cs60409h.

6. S. Pandey, S. N. Baker, S. Pandey and G. A. Baker, Fluorescent probe studies of polarity and solvation within room temperature ionic liquids: a review, *J. Fluoresc.* 2012, **22**, 1313–1343.

7. V. Armel, J. M. Pringle, M. Forsyth, D. R. MacFarlane, D. L. Officer and P. Wagner, Ionic liquid electrolyte porphyrin dye sensitised solar cells, *Chem. Comm.* 2010, **46**, 3146-3148.

8. P. Cheng, T. Lan, W. Wang, H. Wua, H. Yang, C. Deng, X. Dai and S. Guo, Improved dye-sensitized solar cells by composite ionic liquid electrolyte incorporating layered titanium phosphate, *Solar Energy*, 2010, **84**, 854–859.

9. R. Kawano, T. Katakabe, H. Shimosawa, M. K. Nazeeruddin, M. Grätzel, H. Matsui, T. Kitamura, N. Tanabe and M. Watanabe, Solid-state dye-sensitized solar cells using polymerized ionic liquid electrolyte with platinum-free counter electrode, *Phys. Chem. Chem. Phys.* 2010, **12**, 1916–1921.

10. T. Stergiopoulos, M. Konstantakou and P. Falaras, Dye solar cells combining a TiO_2 surface-blocking organic sensitizer and solvent-free ionic liquid-based redox electrolyte, *RSC Adv.* 2013, **3**, 15014–15021.

11. L-L. Li and E. W-G. Diau, Porphyrin-sensitized solar cells. *Chem. Soc. Rev.* 2013, *4***2**, 291- 304.

12. J. Szmytkowski, T. Bond, M. F. Paige, R. W. J. Scott and R. P. Steer, Spectroscopic and photophysical properties of ZnTPP in a room temperature ionic liquid, *J. Phys. Chem. A* 2010**, 114**, 11471–11476.

13. V. Ermolaev, V. Miluykov, D. Krivolapov, I. Rizvanov, E. Zvereva, S. Katsyuba, O. Sinyashin and R. Shmuzler, Phosphonium ionic liquids based on bulky phosphines: synthesis, structure and properties, *Dalton Trans.,* 2010, **39**, 5564-5571.

14. L. Ferguson and P. Scovazzo, Solubility, diffusivity and permeability of gases in phosphonium-based room temperature ionic liquids: Data and correlations, *Ind. Eng. Chem. Res.* 2007, **46**, 1369-1374.

15. K. J. Fraser and D. R. MacFarlane, Phosphonium-based ionic liquids: an overview, *Aust. J. Chem.* 2009, **62**, 309-321.

16. M. van Burgel, D. A. Wiersma and K. Duppen, The dynamics of one-dimensional excitons in liquids, *J. Chem. Phys.* 1995, **102**, 20-33.

17. J. Moll, S. Daehne, J. R. Durrant and D. A. Wiersma, Optical dynamics of excitons in J aggregates of a carbocyanine dye, *J. Chem. Phys.* 1995, **102**, 6362- 6370.

18. Y. Kitagawa, J. Hiromoto and K. Ishii, Electronic absorption, MCD, and luminescence properties of porphyrin J-aggregates. *J. Porphyrins Phthalocyanines* 2013, **17**, 703–711.

19. N. C. Maiti, S. Mazumdar and N. Periasamy, J- and H-aggregates of porphyrin-surfactant complexes: time-resolved fluorescence and other spectroscopic studies, *J. Phys. Chem. B* 1998**, 102**, 1528-1538.

20. Z. Cao, S. Li and T. Yan, Cation–π interactions between a free-base porphyrin and an ionic liquid: A computational study, *ChemPhysChem* 2012*,* **13**, 1743–1747*.*

21. L. Zhang, Y. Tian and M. Liu, Ionic liquid induced spontaneous symmetry

breaking: emergence of predominant handedness during the self-assembly of tetrakis(4-sulfonatophenyl)porphyrin (TPPS) with achiral ionic liquid, *Phys. Chem. Chem. Phys.* 2011, **13**, 17205–17209.

22. B. R. Danger, K. Bedient, M. Maiti, I. J. Burgess and R. P. Steer, Photophysics of self-assembled zinc porphyrin-bidentate diamine ligand complexes, *J. Phys. Chem. A* 2010**, 114***,* 10960–10968.

23. J. A. O'Brien, S. Rallabandi, U. Tripathy, M. F. Paige and R. P. Steer, Efficient S_2 state production in ZnTPP-PMMA thin films by triplet-triplet annihilation: Evidence of solute aggregation in photon upconversion, *Chem. Phys. Letters* 2009, **475**, 220-222.

24. T. N. Singh-Rachford and F. N. Castellano, Photon Upconversion Based on Sensitized Triplet-Triplet Annihilation. *Coord. Chem. Rev.* 2010, **254**, 2560-2573.

25. M. J. Earle, C. M. Gordon, N. V. Plechkova, K. R. Seddon and T. Welton, Decolorization of ionic liquids for spectroscopy, *Anal. Chem.* 2007, **79**, 758–764. Erratum; 4247.

26. Y. Murakami, H. Kikuchi and K. Kawai, Kinetics of photon upconversion in ionic liquids: energy transfer between sensitizer and emitter molecules, *J. Phys. Chem. B* 2013, **117**, 2487–2494.

27. Y. Murakami, Photochemical photon upconverters with ionic liquids, *Chem. Phys. Letters* 2011, **516**, 56–61.

28. C. Yao, H-B. Kraatz and R. P. Steer, R.P., Photophysics of pyrene-labelled compounds of biophysical interest, *Photochem. Photobiol. Sci.* 2005, 4, 191-199.

29. S. Ogi, K. Sugiyasu, M. Swarup, S. Samitsu and M. Takeuchi, Living supramolecular polymerization realized through a biomimetic approach, *Nature Chem.* 2014, **6**, 188-195.

30. D. K. Lavallee, Kinetics and mechanisms of metalloporphyrin reactions, *Coord. Chem. Rev.* 1985, **61**, 55-96.

31. H. Nagatani and H. Watari, Direct spectrophotometric measurement of demetalation kinetics of 5,10,15,20-tetraphenylporphyrinatozinc(II) at the liquid-liquid interface by a centrifugal liquid membrane method, *Anal. Chem.* 1998, **70**, 2860-2865.

32. M. Gouterman in *The Porphyrins*, ed. D. Dolphin, Academic Press, New York, 1978, vol. 3, p. 1 *ff*.

33. J. S. Baskin, H-Z. Yu and A. H. Zewail, Ultrafast dynamics of porphyrins in the condensed phase: I. Free base tetraphenylporphyrin, *J. Phys. Chem. A* 2002, **106**, 9837-9844.

34. X. Liu, E. K. Y. Yeow, S. Velate and R. P. Steer, Photophysics and spectroscopy of the higher electronic states of zinc metalloporphyrins: a theoretical and experimental study, *Phys. Chem. Chem. Phys.* 2006, **8**, 1298-1309.

35. Y. Kitagawa, J. Hiromoto and K. Ishii, Electronic absorption, MCD, and luminescence properties of porphyrin J-aggregates *J. Porphyrins Phthalocyanines* 2013, **17**, 703–711.

36. H. Matsuzawa, H. Kobayashi and T. Maeda, Spectra and mean association number of porphyrin J aggregate, *Bull. Chem. Soc. Jpn.* 2012, **85**, 774-785.

37. Margalit, R.; Rotenberg, M., Thermodynamics of porphyrin dimerization in

aqueous solutions. *Biochem. J.* **1984**, *219*, 445-450.

38. M. Ali, V. Kumar, S. N. Baker, G. A. Baker and S. Pandey, J-aggregation of ionic liquid solutions of meso-tetrakis(4-sulfonatophenyl)porphyrin, *Phys. Chem. Chem. Phys.* 2010, **12**, 1886-1894.

39. O. Ohno, Y. Kaizu and H. Kobayashi, J-aggregate formation of a water-soluble porphyrin in acidic aqueous media, *J. Chem. Phys.* 1993, **99**, 4128-4139.

40. J. A. Ribo, J. P. Bofill, J. Crusats and R. Rubires, Joint-dipole approximation of the exciton coupling model versus type of bonding and of excitons in porphyrin supramolecular structures, *Chem. Eur. J.* 2001, **7**, 2733-2737.

41. V. S. Chirvony, A. van Hoek , V. A. Galievsky, I. V. Sazanovich, T. J. Schaafsma and D. Holten, Comparative study of the photophysical properties of nonplanar tetraphenylporphyrin and octaethylporphyrin diacids, *J. Phys. Chem. B* 2000**, 104**, 9909-9917.

42. R. D. Bonnett, D. J. McGarvey, A. Harriman, E. J. Land, T. G. Truscott and U. J. Winfield, Photophysical properties of meso-tetraphenylporphyrin and some meso-tetra(hydroxyphenyl)porphyrins, *Photochem. Photobiol.* 1988, **48**, 271-276.

43. H. Kano and T. Kobayashi, Time-resolved fluorescence and absorption spectroscopies of porphyrin J-aggregates, *J. Chem. Phys.* 2002, **116**, 184-195.

44. Y. Gong, J. Xie, A. Xia, X. Shao and Z. Li, Spectroscopic properties of hydrogen-bond-modulated porphyrin dimer in different polar solvents, *J. Lumin.* 2007, **122-123**, 250-252.

45. M-H. Hui and W. R. Ware, Exciplex photophysics. V. The kinetics of fluorescence quenching of anthracene by N,N-dimethylaniline in cyclohexane, *J. Am. Chem. Soc.* 1976, **98**, 4718-4727.

46. M. Y. Choi, J. A. Pollard, M. A. Webb and J. L. McHale, Counterion-dependent excitonic spectra of tetra(*p*-carboxyphenyl)porphyrin aggregates in acidic aqueous solution, *J. Am. Chem. Soc.* 2003, **125**, 810-820.